Journal of Medicinal and Chemical Sciences 6 (2023) 1100-1111

Journal of Medicinal and Chemical Sciences

Journal homepage: http://www.jmchemsci.com/

Original Article

Evaluation of Antibacterial Activity of Iron Oxide Nanoparticles Synthesis by Extracellular *Lactobacillus* against *Pseudomonas Aeruginosa*

Maha Abd Qasim*, Laith Ahmad Yaaqoob

Department of Biotechnology, Science College, University of Baghdad, Baghdad, Iraq

ARTICLE INFO

Article history

Receive: 2022-06-12
Received in revised: 2022-08-16
Accepted: 2022-10-26
Manuscript ID: JMCS-2210-1816
Checked for Plagiarism: **Yes**
Language Editor:
Dr. Nadereh Shirvani
Editor who approved publication:
Dr. Nenad Ignjatovic

DOI:10.26655/JMCHEMSCI.2023.5.15

KEYWORDS

Fe_2O_3 NPs
Antimicrobial activity
Biosynthesis nanoparticles
Pseudomonas aeruginosa
Lactobacillus plantarum
Susceptibility test
Extracellular

ABSTRACT

This study aimed to demonstrate the biosynthetic process of iron oxide nanoparticles (Fe_2O_3-NPs) by using extracellular components produced by environmental isolates of *Lactobacillus plantarum* as reducing and stabilizing agents studied in the laboratory of the university of Baghdad. Add 1 g of iron sulfate to 10 mL of extracellular nanoparticles for synthesis. Biosynthetic Fe_2O_3 nanoparticles have broad application prospects in catalysis, biosensing, anticancer, and biomedicine. Optimal conditions for synthesizing Fe_2O_3 were investigated using UV-VIS, AFM, XRD, FT-IR, and FE-SEM techniques. The UV-VIS wavelength of NPs within the nanoclusters. Susceptibility testing of *P. aeruginosa* showed resistance to tetracycline, trimethoprim-sulfamethoxazole, ceftazidime, and chloramphenicol, whereas sensitive to Amikacin, Norfloxacin, Meropenem, and Ciprofloxacin and the effect of Fe_2O_3 NPs from extracellular component on bacteria *Pseudomonas aeruginosa* on an inhibition zone 18 mm.

GRAPHICAL ABSTRACT

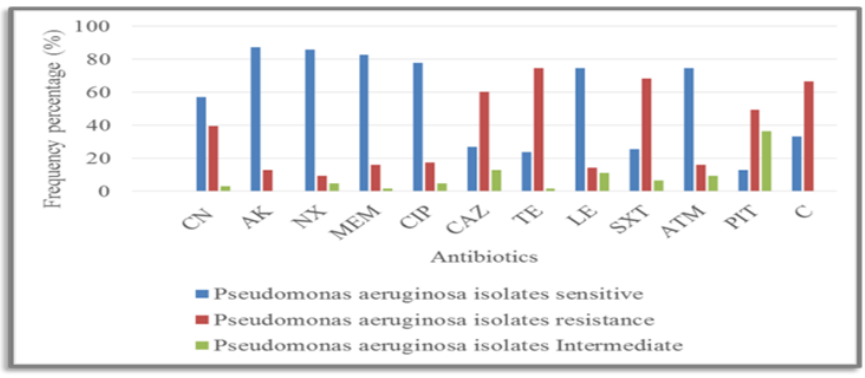

* Corresponding author: Maha A. Qasim
✉ E-mail: Email: maha.abd1206a@sc.uobaghdad.edu.iq

Introduction

The category of *lactobacilli* known as facultatively heterofermentative includes *L. plantarum*. It is a diverse and adaptable species found in a wide range of environmental niches, such as dairy, meat, fish, and numerous plant or vegetable fermentations. Numerous types of cheese have also been reported to contain *L.plantarum* strains. In addition, *L. plantarum* strains have a history of successfully colonizing the intestines of mammals, including humans [1]. *Lactobacillus plantarum* can be distinguished from other bacteria because of its characteristic of Extracellular and Intracellular products; Extracellular and Intracellular are components composed of (Enzymes, proteins, polysaccharides, peptides, pigments, toxins, etc.) [2]. These ingredients act as reducing agents and bioprotectants against various stressors, such as phage attacks, toxic metal ions, and desiccation. These components reduce agents and biological defenses against various stressors such as phage infection, toxic metal ions and desiccation [3]. Iron particles that are smaller than a micron are known as nanoscale iron particles. They have a large surface area, which makes them very reactive. They quickly oxidize to produce free iron ions when oxygen and water are present. They are extensively employed in medical and laboratory applications, and their potential for cleaning up industrial areas contaminated with chlorinated organic chemicals has also been investigated [4]. *Pseudomonas* is a common rod-shaped gram-negative enveloped bacteria that can harm humans, other animals, and plants. Positive for oxidase, catalase, and citrate [5]. *P. aeruginosa*, a species of major medical significance, is an opportunistic bacterium resistant to several medicines and disinfectants that causes severe acute and chronic nosocomial infections in immunocompromised, catheterized, or burn patients [6]. Biofilms are created when bacteria proliferate and attach to the surfaces of biomaterials. The bacterial cells are shielded by the biofilm growth phase from the host defense mechanism and antibiotic [7]. Because of its multitude of scientific and technical uses, including biosensors, iron oxide has attracted particular interest such as antimicrobial activity [8, 9]. Additionally, its biocompatibility and magnetic characteristics have been extensively used in biomedical research [10].

Materials and Methods

Species by taking samples of *Lactobacillus spp* were isolated from a fermented food product. Isolates were cultured in MRS broth, By the manufacturer's instructions [11]. All bacterial species isolate was identified via conventional biochemical assays and procedures through a VITEK2 system.

Extracellular production

Lactobacillus plantarum isolates were grown in MRS broth, incubated at 28 °C for 48 hours, and centrifuged at 8000 rpm for 10 minutes to collect the extracellular solution [12].

Synthesis of iron oxide nanoparticles from the extracellular space

Fe_2O_3 nanoparticles were synthesized by a modified biosynthetic method (biological synthesis method) using iron sulfate $Fe_2(SO_4)_3$ (India) to generate iron oxide nanoparticles from extracellular for *Lactobacillus SPP*. [13]. Typical procedure: Dissolve 5 g of ferric sulfate $Fe_2(SO_4)_3$ in 50 mL of *Lactobacillus SPP* extracellular product solution, dispersed by an ultrasonication bath for 10 min to more mix component and kept in the dark condition overnight on the shaker. The resulting solution was centrifuged at 8000 rpm for 10 minutes and washed twice with deionized distilled water to remove residual extracellular cells. It was then dried in an oven at 40°C overnight to obtain a brown powder and stored in the dark for later use.

Pseudomonas aeruginosa isolate

The clinical specimens of *P.aeruginosa* collection are 121 clinical isolates and took place from burns and wounds from November 2021 to January 2022. It is important to note that the samples contain burns and wounds. Under the specific condition, Cetrimide agar prepared according to the manufacturer was used to streak specimens taken from the hospital (Al Shula

Teaching, Al-Kadmia Teaching, and Baghdad/Medical City) [14]. Other identification tests included biochemical and morphological characteristics, and the Vitek-2 system was performed [15].

Antibacterial activity of Fe_2O_3 Nanoparticles

Pseudomonas aeruginosa was cultured on Muller-Hinton agar and using the good method (MIC) of microbial inhibition by using Fe_2O_3 NPs synthesis from extracellular sources [16].

Detection of Biofilm (quantitative method)

After incubating the *P. aeruginosa* isolates in BHI medium at 37 °C for 24 hours, added (200 µl) of *P.aeurginosa* broth was to each well in a microtiter plate, and then (200 µl) of BHI medium was added to each well in a microtiter plate. After the incubation period, each well was washed three times with phosphate-buffered saline. Plates were then air-dried at room temperature for 15 minutes before adding 99% methanol (200 µL) over 15 minutes. Plates were then air-dried at room temperature for 15 minutes and stained with 200 µl of 2% crystal violet for approximately 15 minutes. After completely removing the stain, add 200 µL of 95% ethanol to each stained well and incubate at room temperature for 15 minutes. The optical density of the plate's wells was measured using a micro-ELISA auto reader at 520nm. Then they used Sterile BHI broth as a negative control of the test. To compensate for background absorbance, the mean of (OD) is optical density, and the reading value of the control mean (C) was taken from the test (T) values [17]. Table 1 measures the intensity of biofilm:

Table 1: Intensity of biofilm

Adherence of Biofilm Formation	Interpretation
ODs ≤ ODc	Non-adherent
ODc < ODs ≤ 2 * ODc	Weakly adherent
2 * ODc < ODs ≤ 4 * ODc	Moderately adherent
4 * ODc < ODs	Strongly adherent

Results and Discussion

Bacterial isolation in culture media

Lactobacilli samples were obtained from various sources, including dairy products (milk, buffalo, cheese, yogurt*)* [18]. The samples were cultured on MRS agar plates as selective media for isolation and incubated at 28 °C for 48 hours with the presence of (3-5 %) CO_2 using Candle Jar. These bacteria can be examined using morphology, microscopy, and biochemistry testing to validate their identity (Figure 1).

Antibiotic susceptibility test of P.aeruginosa

Of the 121 isolates, only 63 were tested for susceptibility to 12 different antibiotics using the disc diffusion method recommended by the Clinical and Laboratory Standards Institute (CLSI, 2021) [19]. Guidelines and the results shown in Figure 2 showed varying levels of resistance; in this study, *P.aeruginosa* showed the highest percent of resistance to tetracycline, followed by Trimethoprim-Sulfamethoxazole, Ceftazidime, and Chloramphenicol.

Absorption maxima were detected in extracellular applications using a UV-Vis spectrophotometer (Shimadzu, Japan) developed from *Lactobacillus plantarum* [20]. Figure 3 Shows extracellular absorption at 289 nm.

Characterization of biological synthesis Fe_2O_3 NPs

UV–VIs spectral analysis Fe_2O_3 from extracellular

The optical properties of the nanoparticles were studied by exploiting ultraviolet – Visible spectrometer. Figure 4 shows the absorbance of the sample in the nano range at room temperature. It has shown a peak at 290 nm wavelength was thus agreed with [21].

Figure 1: *Lactobacillus plantarum* cultured on MRS agar

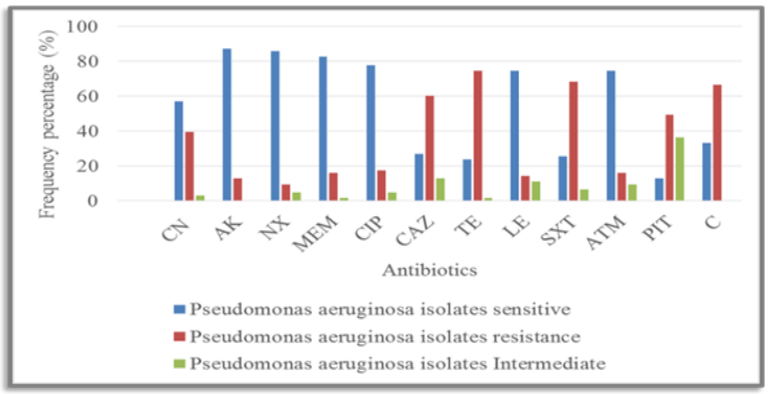

Figure 2: The results of antibiotic susceptibility test of *P.aeruginosa*

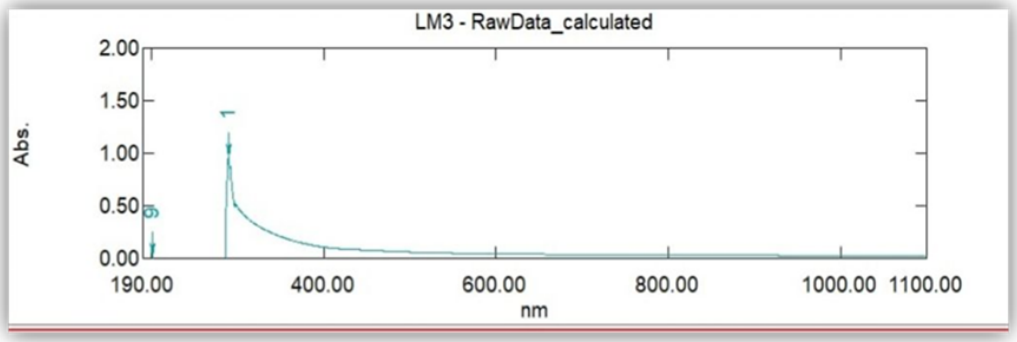

Figure 3: The UV-VIs of extracellular

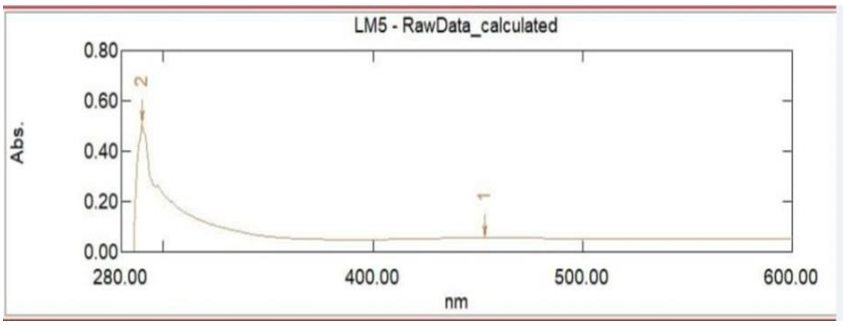

Figure 4: The UV-VIS of Fe_2O_3 nanoparticles synthesis using extracellular

Atomic force microscopy (AFM) analysis of Fe_2O_3 from extracellular

The surface shape formation of the Fe_2O_3 NPs was studied by atomic force microscopy to show that Fe_2O_3 NPs 2D and 3D (Figure 5) [22]. AFM images show that the biosynthesized Fe_2O_3 NPs are spherical. The size of an average diameter of 31.34 nm (Table 2) was also measured by AFM (Figure 6).

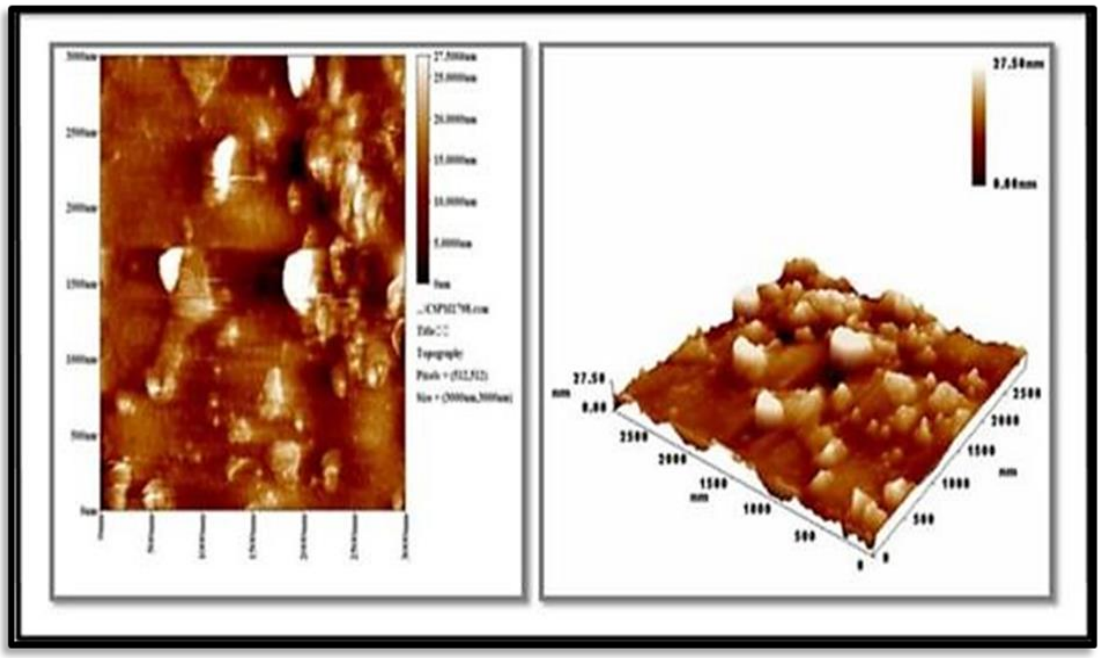

(2D) **(3D)**

Figure 5: Atomic force microscopy (AFM) of Fe_2O_3 NPs synthesized using extracellular illustrate2D and 3D topological

Table2: The average diameter of Fe_2O_3 nanoparticles synthesized using extracellular

Avg. Diameter: 31.34 nm	<=10% Diameter: 14.00 nm
<=50% Diameter: 28.00 nm	<=90% Diameter: 50.00 nm

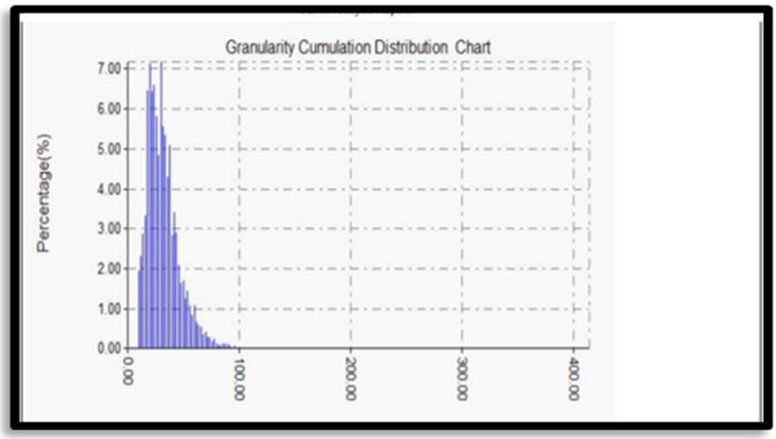

Figure 6: The average size of iron nanoparticles synthesized using extracellular

Fourier transform infrared (FT-IR) analysis of Fe_2O_3 from extracellular

FT-IR spectrum has determined the functional groups of nanoparticles. Figure 7 represents the absorption spectrum of biologically synthesized nanoparticles in FT-IR. An intense peak at

3398.34 cm^{-1} was visible due to OH stretching mode. The peak properties at 1629.74 cm^{-1} suggested the presence of crystallographic H_2O molecules, i.e., O–H bend. The wide peak at 455,17 cm^{-1} and 572,82 cm^{-1}, respectively, represented the Fe–O band and Fe–O–Fe skeletal frequency [13].

X-Ray diffractometer analysis of Fe_2O_3 from extracellular

The X-ray deviation examination was performed to define the surface Morphology and the composition of the crystals Of Fe_2O_3 NPs, including crystalline size, lattice parameters, the thickness of the crystal, and textile factor. X-ray bias results for the Fe_2O_3 model calibrated to typical data from the Joint Commission Powder Diffraction Standard (JCPDS) #11-0614. X-ray diffraction test results for Fe_2O_3 NPs include declination and declination data format. The bias model was created using Origin 9.0 for Windows operating system (Figure 8). Deviation patterns are: It has seven diffraction peaks. The seven diffraction peaks represent electron diffraction processes occurring in the Fe_2O_3 nanoparticle diffraction planes, namely fields (220), (311), (400), (422), (511), (440), and (533). The diffraction pattern characteristic of Fe_3O_4 nanoparticles is according to JCPDS-11-0614 standard data [23, 24]. Similar to nanomaterials, particle size decreases with increasing peak width. Crystal structure parameters were obtained at b=0.3785 nm and c=0.9513 nm. The average crystallite size was calculated using the Debye-Scherrer equation [25]. The results show that the crystallographic planes (θ = diffraction angle) of Fe_2O_3 are 30.10°, 35.51°, 45.21°, 53, 44° and 57.31°, respectively, with six obvious strong diffraction peaks. 2θ and 62.81° are observed.

Field emission scanning electron microscopy analysis of Fe_2O_3 from extracellular

Through applying FE-SEM, images were taken of the sample at a magnification of 50kx. Focused on Figure 9. The whole sample has soft planes and a uniform shape in the form of Fe_2O_3 nanocluster centers [13].

Antibacterial susceptibility test

Iron oxide NPs antibacterial activity was investigated using Gram-negative bacteria (*Pseudomonas aeruginosa*). The minimum inhibitory concentration (MIC) of Fe_2O_3 NPs against microorganisms was calculated using the agar well diffusion method [26, 27].

Pour approximately 25 mL of sterile Mueller Hinton Agar into a sterile plate and let it to come to room temperature. Wells were prepared by transferring the growth of the test species onto agar and isolating the wells by pinching a sterile cotton swab. Then different ratios of Fe_2O_3 NPs from extracellular (500, 250, 125, 62.5, 31.25, 15.625, 7.8125, 3.90625, 1.953125) mg/mL. Plates seeded with Fe_2O_3 NPs were incubated at 37 °C for 24 hours. Assess the zone of inhibition around the well after incubation [13]. Results of Fe_2O_3 NPs from extracellular antibacterial activity were demonstrated in (Figure 10). The antibacterial activity was found to be directly dependent upon the Fe_2O_3 NPs concentration. Table 3 shows that at a concentration of 500 mg/mL Fe_2O_3-NPs from extracellular material, the maximum inhibition zone of *P. aeruginosa* was 18 mm, while the minimum inhibition zone was 15.625 mg/mL Fe_2O_3 NPs concentration. The difference in inhibitory diameter may be due to the different interactions between Fe_2O_3 NPs and microorganisms and the different susceptibility of the bacteria used in the current study. The main mechanism of toxicity of Fe_2O_3 NPs potentially associated with metal oxides carries the positive charge even though the microorganisms bear negative charges; this results in electromagnetic interaction between microorganisms and metal oxides, leading to oxidation and, finally, death of microorganisms. Extracellular Fe_2O_3 NPs were found to have MICs ranging from 500 to 1.953125 mg/mL by serial dilution methods described in CLSI [13]. The bactericidal action of Fe_2O_3 nanoparticles on bacteria is of extreme importance due to the ability of pathogenic bacteria to join the ecosystem's food chain [28]. The antibacterial effect of Fe_2O_3 on bacteria was confirmed [28] and communicated in modern research.

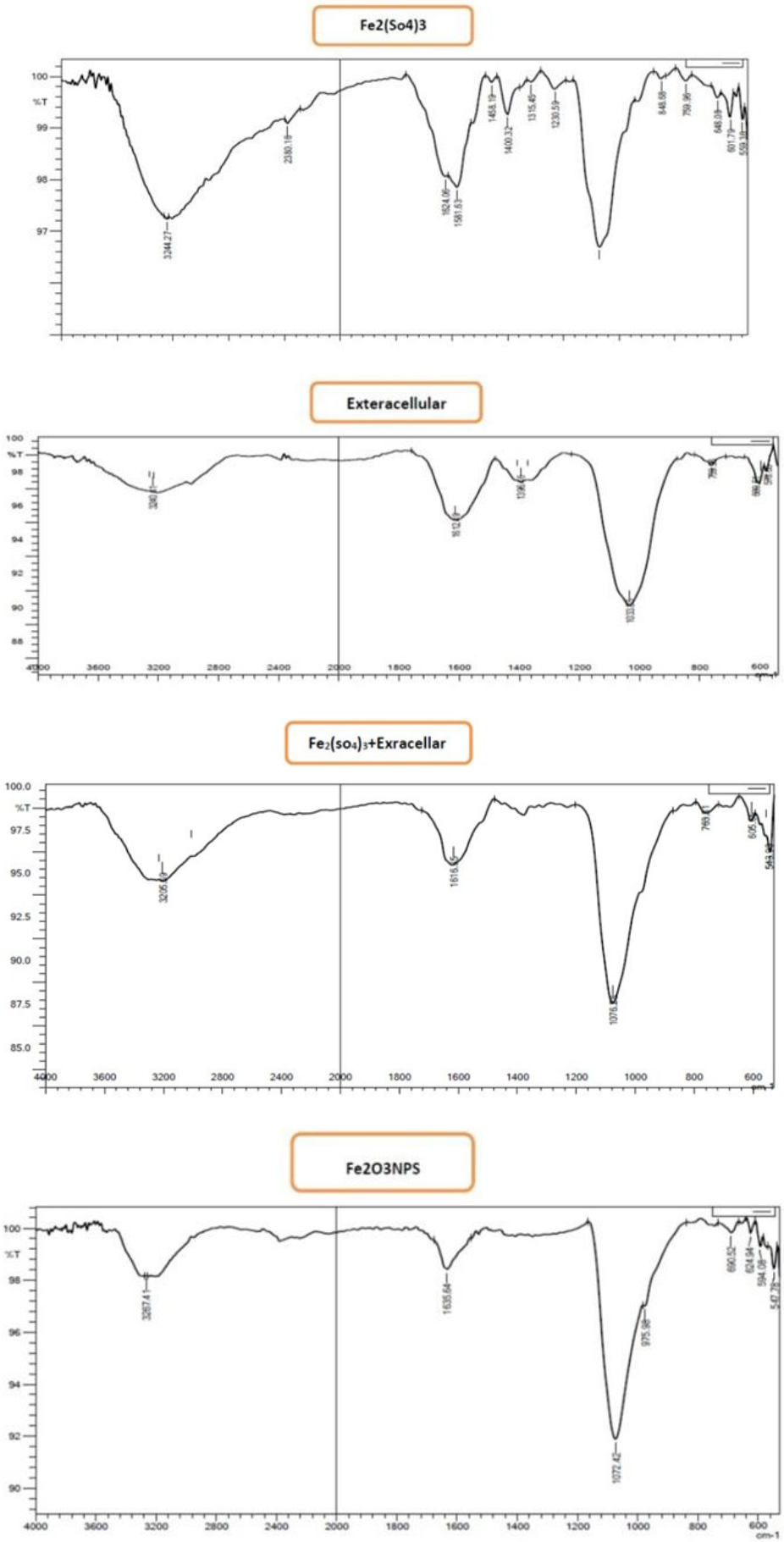

Figure 7: FT-IR image of Fe_2O_3 NPs synthesized using extracellular (A) $Fe_2(SO_4)_3$, (B) extracellular, (C) $Fe_2(SO_4)_3$-extracellular, (D) Fe_2O_3NPs

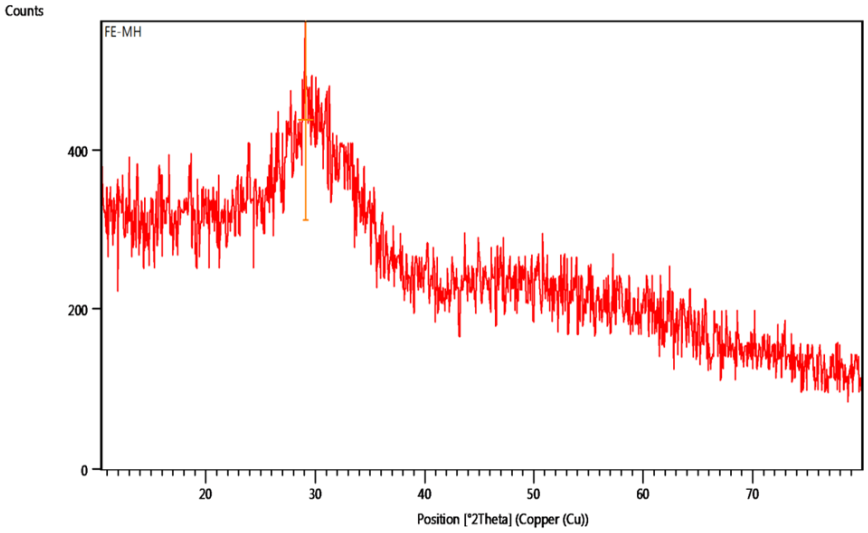

Figure 8: XRD Pattern of Fe_2O_3 NPs synthesized using extracellular

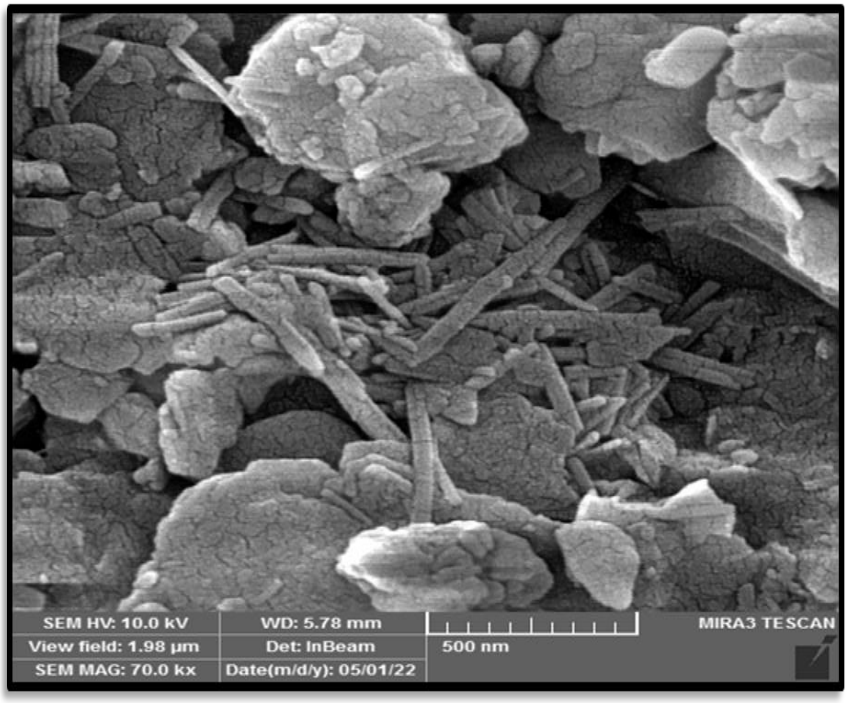

Figure 9: FE-SEM images of Fe_2O_3 NPs synthesized using extracellular

Detection of biofilm production by microtiter plate assay

Under the same experimental conditions, all 20 *Pseudomonas aeruginosa* isolates showed different potential biofilm-forming abilities (Figure 11). Separation results were limited to three groups. Six isolates were high biofilm producers (30%), seven isolates were intermediate biofilm producers (35%), and seven isolates were low biofilm producers (35%). These results were obtained after 24 hours of incubation of *Pseudomonas aeruginosa* growth and biofilm formation.

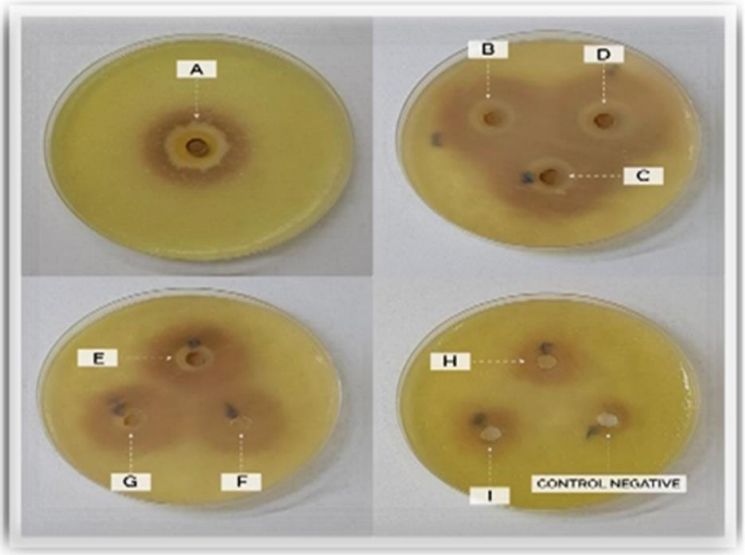

Figure 10: Antibacterial activity of Fe_2O_3 NPs from extracellular on *P.aeruginosa*

Table 3: The inhibition zone of antibacterial effect of Fe_2O_3 from extracellular on *P.aeruginosa*

Fe_2O_3 concentration (mg/mL)		Inhibition zone (mm)
A	500	18
B	250	16
C	125	15
D	62.5	14
E	31.25	11
F	15.625	10
G	7.8125	Nill
H	3.90625	Nill
I	1.953125	Nill

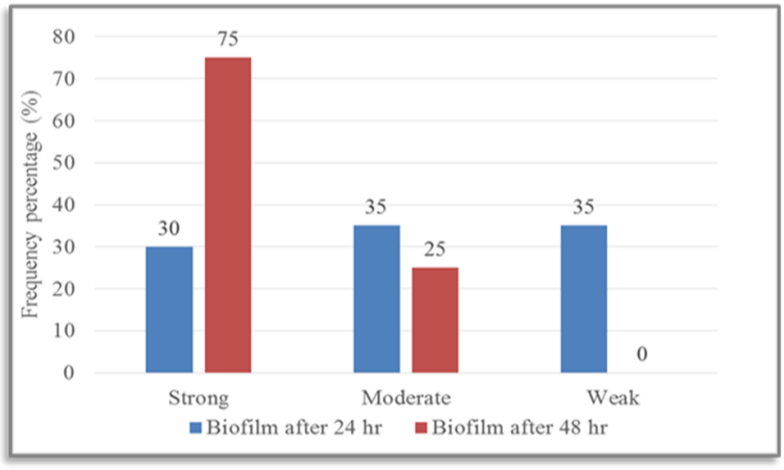

Figure 11: biofilm formation of *Pseudomonas aeruginosa* after 24 h and 48 h

After 48 hours of incubation, 20 isolates were tested in microtiter plates. It shows that 15 isolates (75%) are strong biofilm producers, five isolates (25%) are moderate biofilm producers and 0 isolates (0%) are weak biofilm producers.

Conclusion

This study demonstrated the biosynthesis of iron oxide nanoparticles using extracellular as a reducing agent. Additionally, the attained Fe_2O_3 NPs were characterized using UV-Vis, AFM, XRD,

FT-IR, and FE-SEM techniques. In particular, The XRD patterns showed the successful Fe_2O_3 NPs phase formation.

At the same time, the FE-SEM demonstrated that the prepared Fe_2O_3 NP exhibited spherical particles and plate-like structures with an average diameter size ranging between 30-50 nm. In contrast, the AFM revealed an average diameter of 31.34 nm. The antibacterial activity test found that the bio-synthesized has a strong antibacterial activity against the introduced bacteria. The maximum inhibition zone was found to be 18 mm at a concentration of 500 mg/Ml.

Funding

This research did not receive any specific grant from funding agencies in the public, commercial, or not-for-profit sectors.

Authors' contributions

All authors contributed to data analysis, drafting, and revising of the paper and agreed to be responsible for all the aspects of this work.

Conflict of Interest

The author declared that they have no conflict of interest.

References

[1]. Zago M., Fornasari M.E., Carminati D., Burns P., Suàrez V., Vinderola G., Reinheimer J., Giraffa G., Characterization and probiotic potential of Lactobacillus plantarum strains isolated from cheeses, *Food Microbiology*, 2011, **28**:1033 [Crossref], [Google Scholar], [Publisher]

[2]. Li S., Tang S., He Q., Hu J., Zheng J., Changes in proteolysis in fermented milk produced by Streptococcus thermophilus in co-culture with Lactobacillus plantarum or Bifidobacterium animalis subsp. lactis during refrigerated storage, *Molecules*, 2019, **24**:3699 [Crossref], [Google Scholar], [Publisher]

[3]. Kanmani P., Satish Kumar R., Yuvaraj N., Paari K.A., Pattukumar V., Arul V., Probiotics and its functionally valuable products—a review, *Critical reviews in food science and nutrition*, 2013, **53**:641 [Crossref], [Google Scholar], [Publisher]

[4]. Zhang W.X., Nanoscale iron particles for environmental remediation: an overview, *Journal of nanoparticle Research*, 2003, **5**:323 [Crossref], [Google Scholar], [Publisher]

[5]. Morales-López S., Yepes J.A., Prada-Herrera J.C., Torres-Jiménez A., Enterobacteria in the 21st century: A review focused on taxonomic changes, *The Journal of Infection in Developing Countries*, 2019, **13**:265 [Crossref], [Google Scholar], [Publisher]

[6]. Behzadi P., Baráth Z., Gajdács M., It's not easy being green: a narrative review on the microbiology, virulence and therapeutic prospects of multidrug-resistant Pseudomonas aeruginosa, *Antibiotics*, 2021, **10**:42 [Crossref], [Google Scholar], [Publisher]

[7]. Obaid S.A., Al-Shwaikh R.M., Evaluation the Efficacy of Bacteriophage Against Pseudomonas Aeruginosa Isolated from Wound and Burn Infections. Paki*stan Journal of Medical & Health Sciences*. 2022, **16**:440 [Crossref], [Google Scholar], [Publisher]

[8]. Urbanova V., Magro M., Gedanken A., Baratella D., Vianello F., Zboril R., Nanocrystalline iron oxides, composites, and related materials as a platform for electrochemical, magnetic, and chemical biosensors, *Chemistry of Materials*, 2014, **26**:6653 [Crossref], [Google Scholar], [Publisher]

[9]. Balouiri M., Sadiki M., Ibnsouda S.K., Methods for in vitro evaluating antimicrobial activity: A review, *Journal of pharmaceutical analysis*, 2016, **6**:71 [Crossref], [Google Scholar], [Publisher]

[10]. Ganapathe L.S., Mohamed M.A., Mohamad Yunus R., Berhanuddin D.D., Magnetite (Fe3O4) nanoparticles in biomedical application: From synthesis to surface functionalization, *Magnetochemistry*, 2020, **6**:68 [Crossref], [Google Scholar], [Publisher]

[11]. Yeong M.S., Hee M.S., Choon C.H., Characterization of high-ornithine-producing Weissella koreensis DB1 isolated from kimchi and its application in rice bran fermentation as a starter culture, *Foods*, 2020, **9**:1545 [Crossref], [Google Scholar], [Publisher]

[12]. Lee I.C., Caggianiello G., van Swam I.I., Taverne N., Meijerink M., Bron P.A., Spano G., Kleerebezem M., Strain-specific features of extracellular polysaccharides and their impact on Lactobacillus plantarum-host interactions, *Applied and environmental microbiology*, 2016, **82**:3959 [Crossref], [Google Scholar], [Publisher]
[13]. Yaaqoob L.A., Evaluation of the Biological Effect Synthesized Iron Oxide Nanoparticles on Enterococcus Faecalis, Iraqi Journal of Agricultural Sciences, 2022, **53**:440 [Crossref], [Google Scholar], [Publisher]
[14]. Ali R.H., Majeed M.R., Jasim H.A., Determination of vasicine alkaloid efficacy as inhibitor to the activity of protease produced by a clinical isolate of Pseudomonas aeruginosa. *Iraqi Journal of Science*, 2018 **29**:1237 [Crossref], [Google Scholar], [Publisher]
[15]. Gavin P.J., Warren J.R., Obias A.A., Collins S.M., Peterson L.R., Evaluation of the Vitek 2 system for rapid identification of clinical isolates of gram-negative bacilli and members of the family Streptococcaceae, *European Journal of Clinical Microbiology and Infectious Diseases*, 2002, **21**:869 [Crossref], [Google Scholar], [Publisher]
[16]. Prodan A.M., Iconaru S.L., Chifiriuc C.M., Bleotu C., Ciobanu C.S., Motelica-Heino M., Sizaret S., Predoi D., Magnetic properties and biological activity evaluation of iron oxide nanoparticle, *Journal of nanomaterials*, 2013, **2013**:893970 [Crossref], [Google Scholar], [Publisher]
[17]. Djordjevic D., Wiedmann M., McLandsborough L.A., Microtiter plate assay for assessment of Listeria monocytogenes biofilm formation, *Applied and environmental microbiology*, 2002, **68**:2950 [Crossref], [Google Scholar], [Publisher]
[18]. Oyetayo V.O., Phenotypic characterisation and assessment of the inhibitory potential of Lactobacillus isolates from different sources, *African journal of biotechnology*, 2004, **3**:355 [Crossref], [Google Scholar], [Publisher]
[19]. Nyuykonge B., Van Amelsvoort L., Eadie K., Fahal A.H., Verbon A., Van De Sande W., Comparison of Disc Diffusion, Etest, and a Modified CLSI Broth Microdilution Method for In Vitro Susceptibility Testing of Itraconazole, Posaconazole, and Voriconazole against Madurella mycetomatis, *Antimicrobial Agents and Chemotherapy*, 2021, **65**:e00433 [Crossref], [Google Scholar], [Publisher]
[20]. Dhoondia Z.H., Chakraborty H., Lactobacillus mediated synthesis of silver oxide nanoparticles, *Nanomaterials and nanotechnology*, 2012, **2**:15 [Crossref], [Google Scholar], [Publisher]
[21]. Aparicio-Caamaño M., Carrillo-Morales M., Olivares-Trejo J.J., Iron oxide nanoparticle improves the antibacterial activity of erythromycin, *Journal of Bacteriology and Parasitology*, 2016, **7**:2 [Crossref], [Google Scholar], [Publisher]
[22]. Abdul Hassan M.M., Hassan S.S., Hassan A.K., Comparative of Green-Synthesis of Bimetallic Nanoparticles Iron/Nickel (Fe/Ni) and Supported on Zeolite 5A: Heterogeneous Fenton-like For Dye Removal From Aqueous Solutions. *Asian Journal of Water, Environment and Pollution*, 2022, **19**:53 [Crossref], [Google Scholar], [Publisher]
[23]. Machado I., Graça J., Lopes H., Lopes S., Pereira M.O., Antimicrobial pressure of ciprofloxacin and gentamicin on biofilm development by an endoscope-isolated Pseudomonas aeruginosa, *International Scholarly Research Notices*, 2013, **2013**:178646 [Crossref], [Google Scholar], [Publisher]
[24]. Malega F., Indrayana I.P., Suharyadi E., Synthesis and characterization of the microstructure and functional group bond of fe3o4 nanoparticles from natural iron sand in Tobelo North Halmahera, *Jurnal ilmiah pendidikan fisika Al-Biruni*. 2018, **7**:13 [Crossref], [Google Scholar], [Publisher]
[25]. Zhang L., Webster T.J., Nanotechnology and nanomaterials: promises for improved tissue regeneration, *Nano today*, 2009, **4**:66 [Crossref], [Google Scholar], [Publisher]
[26]. Christian P., Von der Kammer F., Baalousha M., Hofmann T., Nanoparticles: structure, properties, preparation and behaviour in environmental media, *Ecotoxicology*, 2008, **17**:326 [Crossref], [Google Scholar], [Publisher]
[27]. Mahdavi M., Namvar F., Ahmad M.B., Mohamad R., Green biosynthesis and characterization of magnetic iron oxide (Fe3O4)

nanoparticles using seaweed (Sargassum muticum) aqueous extract, *Molecules*, 2013, **18**:5954 [Crossref], [Google Scholar], [Publisher]

[28]. Stoimenov P.K., Klinger R.L., Marchin G.L., Klabunde K.J., Metal oxide nanoparticles as bactericidal agents, *Langmuir*, 2002, **18**:6679 [Crossref], [Google Scholar], [Publisher]

HOW TO CITE THIS ARTICLE
Maha A. Qasim, Laith Ahmad Yaaqoob. Evaluation of Antibacterial Activity of Iron Oxide Nanoparticles Synthesis by Extracellular Lactobacillus against Pseudomonas Aeruginosa. *J. Med. Chem. Sci*., 2023, 6(5) 1100-1111
https://doi.org/10.26655/JMCHEMSCI.2023.5.15
URL: http://www.jmchemsci.com/article_159625.html